



Journal of Mining and Environment (JME)

journal homepage: www.jme.shahroodut.ac.ir



Identification of Buried Metal Ore Deposits using Geochemical Anomaly Filtering and Principal Factors of Power Spectrum

Hossein Mahdianfar*

Department of Mining Engineering, University of Gonabad, Gonabad, Iran

Article Info

Received 29 September 2020

Received in Revised form 01 December 2020

Accepted 7 December 2020

Published online 7 December 2020

DOI:10.22044/jme.2020.10114.1949

Keywords

Geochemical anomaly filtering

Buried deposit

Wavenumber-Based filter

Power spectrum

Abstract

Over the past two decades, the frequency domain (FD) of the geochemical data has been studied by some researchers. Metal zoning is one of the challenging subjects in the mining exploration, where a new scenario has been proposed for solving this problem in FD. Three mineralization areas including the Dalli (Cu-Au), Zafarghand (Cu-Mo), and Tanurcheh (Au-Cu) mineralization areas are selected for this investigation. After transferring the surface geochemical data to FD, the geochemical signals obtained are filtered using the wavenumber-based filters. The high and moderate frequency signals are removed, and the residual signals are interpreted by the statistical method of principal component analysis (PCA). In order to discriminate the deep metal ore deposits, the principal factors of elemental power spectrum extracted by PCA are depicted in a novel diagram (PC1 vs. PC2). This approach indicates that the geochemical data in the Dalli and Zafarghand deep ore deposits have similar frequency behaviors. The Au, Mo, and Cu elements in these two areas are discriminated from the Au, Mo, and Cu mineralization elements of the Tanurcheh area as a deep non-mineralization zone in this diagram. This new criterion used for distinguishing the buried ore deposits and deep non-mineralization zones is properly confirmed by the exploratory deep drilled boreholes. The geochemical anomaly filtering demonstrates that the strong signatures of deep mineralization are associated with the low frequency geochemical signals at the surface, and the buried mineralization areas with weak surface anomaly can be identified using the geochemical FD data.

1. Introduction

Interpretation of the geochemical data is an essential stage in the mining exploration. The geochemical data is interpreted in three important domains including the spatial, frequency, and position-scale domains. The geochemical data can be transferred to the frequency domain (FD) using Fourier transformation (FT). FT, as a data mining approach, has been frequently utilized in various significant fields such as gravity and magnetic data in the geophysics, remote sensing, signal processing, data compression, and image processing [1]. Cheng *et al.* (1999, 2000) have applied the power spectrum (PS) values of the geochemical data for separating the geochemical anomaly, background, and noise components at the

first time [2, 3]. They extended the concentration-area fractal method in FD, and proposed the power spectrum-area (S-A) fractal method for anomaly separation. The fractal/multi-fractal modeling methods have been applied in order to recognize the geochemical anomalies [4, 5]. The S-A fractal method has been applied for separation of the geochemical background from the anomaly in FD [6-13]. Zuo (2011) has utilized the principal component analysis (PCA) and the S-A fractal method for separation of the Cu, Pb, and Ag geochemical anomaly [14]. Wang and Zuo (2015) have accomplished the trend surface and fractal analysis for separating the anomaly area in FD of geochemistry [15]. The power spectrum-volume

✉ Corresponding author: Hssn.shahi@gmail.com (H. Mahdianfar).

fractal method has been used in order to identify the mineralization zones such as the supergene and hypogene zones in FD [16, 17].

Shahi *et al.* (2016, 2015) have achieved new information about the Cu deep mineralization, predicting the mineralization zones at various depths using FD of the surface geochemical data [18, 19]. They have demonstrated that the deep ore deposits, the same as the background elements, create weak geochemical concentrations at the surface containing low-frequency geochemical signals that can be distinguished using the spectral analysis of the geochemical data. They predicted the variability of mineralization from the surface to the depth by interpretation of the PS values of the mineralization elements. FD of the geochemical data has also been applied in order to distinguish the deep mineralized and non-mineralized zones [20].

Various studies have been performed on FD of the geochemical data in order to detect the geochemical patterns. New exploratory information about the presence or absence of metal ore deposits at the depth can be extracted from the surface geochemical frequency signals.

In this investigation, the geochemical anomaly filtering in three mineralization areas (Dalli Cu-Au mineralization area, Zafarghand Cu-Mo mineralization area, and Tanurcheh Au-Cu mineralization area) was performed using the wavenumber-based filters, and the geochemical signals were interpreted using PCA. PCA and robust PCA were performed for enhancement of

the multivariate geochemical anomalies, dimension reduction of variables, detection of data structure, and prediction of hidden geochemical patterns [10, 16, 21, 22]. Recognizing the significant geological factors and the mineralization process is an important issue in mineral exploration [23, 24]. In this work, the PCA method was performed in order to determine the geological and mineralization factors involved in FD.

PCA, as a multivariate statistical method, can determine the relationship between the elements on the basis of the correlation coefficients or covariance. PCA reduces the dimensionality of a multivariate data set and summarizes the information by creating a smaller numbers of new variables named the principal components (PCs) based on the initial variables [25]. The interrelated variables create PCs that are uncorrelated. The first PC includes the greatest variance of the dataset [26].

2. Power spectrum of geochemical data

Joseph Fourier has indicated that the spatial and temporal functions can be decomposed into the simple sinusoidal functions using a mathematical tool named FT. 2D-FT, as a data mining method, converts 2D spatial data such as images to FD [27]. A variety of simple frequency signals are extracted from the spatial and temporal functions using the following equation [28]:

$$F(K_x, K_y) = \int_{-\infty}^{\infty} \int_{-\infty}^{\infty} f(x, y) \cos(K_x x + K_y y) dx dy - i \int_{-\infty}^{\infty} \int_{-\infty}^{\infty} f(x, y) \sin(K_x x + K_y y) dx dy \quad (1)$$

This equation can be used to calculate the function $F(K_x, K_y)$ in FD based on the 2D $f(x, y)$ spatial function. K_x and K_y are “wave numbers” on the basis of the x and y axes. The wave numbers correspond to the frequency values, and hold a direct relationship with the wavelengths as bellow:

$$\lambda_x = 2\pi / K_x \text{ and } \lambda_y = 2\pi / K_y,$$

or (2)

$$\lambda = 2\pi \sqrt{(1/K_x^2 + 1/K_y^2)}$$

FT can be used to calculate the real, $R(K_x, K_y)$, and imaginary, $I(K_x, K_y)$, components of the signals. The PS values can be obtained on the basis of the following equation:

$$E(K_x, K_y) = R^2(K_x, K_y) + I^2(K_x, K_y) \quad (3)$$

The geochemical maps include superimposed signals with different frequencies [2]. The Fourier method, as a powerful technique, has been applied to transfer the geochemical data to FD. In the first step, the geochemical distribution map should be depicted using the conventional interpolation methods such as the Kriging and inverse distance weighted methods. The geochemical interpolated map obtained is considered as the 2D $f(x, y)$ function, and FT is accomplished on this spatial map. Therefore, the geochemical map can be converted into the $F(K_x, K_y)$ function in FD that provides the K_x - K_y map consisting of the PS and phase spectrum values. The spectral maps obtained, which show the distribution of geochemical frequency signals, can be interpreted

using various methods such as the fractal and statistical methods in FD [29].

3. Case studies

In this research work, three mineralization areas, as the case studies, were selected and applied for discussion. These areas include the Dalli Cu-Au mineralization area, Zafarghand Cu-Mo mineralization area, and Tanurcheh Au-Cu mineralization area, all located in Iran (Figure 1). The hidden mineralization zones have been explored at the depth in the Dalli and Zafarghand areas so that these areas are known as the economic buried mineralization zones. The drilled boreholes do not show notable mineralization zones at the depth in the Tanurcheh area. These three mineralization areas were utilized in order to characterize the deep non-mineralization and mineralization zones using the frequency features of the geochemical elements.

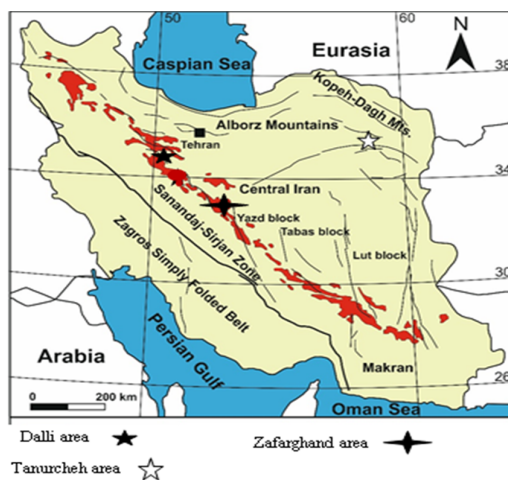


Figure 1. Location of the studied areas in the map of Iran.

3.1. Dalli Cu-Au porphyry mineralization area

The Dalli area is located in the Uremia–Dokhtar magmatic belt in the central Iran [30]. The copper-gold mineralization of the Dalli area has been formed in the dacite, andesite, porphyritic amphibole andesite, diorite, and quartz diorite porphyry rocks [30, 31]. Various alterations consisting of potassic, sericitic, sericite–chlorite, propylitic, and silicic are seen in this area. The alterations of potassic and quartz–sericite are related to the gold-copper mineralization. The mineralization includes the stockworks of quartz, Chalcopyrite, pyrite, bornite, magnetite, malachite, and iron oxides [30].

3.2. Zafarghand Cu-Mo porphyry deposit

The Zafarghand area is also located in the Urumieh–Dokhtar magmatic belt. There is a strong porphyry alteration system (7 km²) in this area, and dacite, rhyolite dacite porphyry, quartz diorite, andesite porphyry, and diorite porphyries have been strongly altered to potassic, phyllic, argillic, and propylitic. The mineralization includes quartz-magnetite stockworks, quartz veins, chalcopyrite, pyrite, galena, sphalerite, malachite, and iron oxides. Some mineralization elements can be seen in the silicified quartz veins [32]. The readers are referred to Shahi *et al.* (2016) [19] for further information.

3.3. Tanurcheh Cu-Au porphyry mineralization area

The Tanurcheh area is located in the Khaf-Daruneh geological belt in the northeast of Iran. The major lithological units include pyroclastic, lavas, and intrusive igneous rocks. The pyroclastic rocks mainly consist of tuff, lapilli-tuff, and crystal-tuff. The intrusive igneous rocks consist of porphyry-monzonite, quartz-monzonite, and porphyry-diorite. The latite rocks have a porphyry texture, and their major alteration is silicification. Secondary iron oxides are usually in the veins and veinlets forms, and brecciated or disseminated zones. The veinlets of stock-work, semi-parallel veinlets with secondary iron oxides, are located in the phyllic alteration zone. The secondary iron oxides such as hematite, goethite, and limonite are distributed over the altered area of Tanurcheh, and can be the result of oxidization of sulfide minerals. In addition to silicification at different parts of the Tanurcheh area, a complex of silica veins and veinlets enriched with the secondary iron oxides has also been developed. Mineralization within silica is in the form of vuggy quartz type with fine pyrite disseminated in the rock texture. The pyrites in the later phases appear with the veins, veinlets, and breccias, and are associated with the secondary iron oxides mainly in the form of goethite [34].

4. Frequency behavior of elements in buried mineral deposits

Exploring the buried and deep ore deposits is an important priority in the exploratory geochemistry. Understanding the geological and structural features, geochemical migration processes, and behavior of mineralization elements in the spatial domain and FD can help us to identify the buried ore deposits with a weak surface geochemical anomaly. Cheng (2014) has mathematically

characterized the decreasing rate of element concentration from the depth to the surface. He has demonstrated that there is a non-linear relationship between the mineralization element concentration and the vertical distance from the buried ore deposit that has been caused due to regolith, geochemical barriers, and complicated migration processes. The mineralization elements of deep ore deposits with thick overburden layers may hold very weak concentrations at the surface [35]. The buried ore deposits create weak geochemical signals at the surface due to the regolith and overburden layers, and hence, discrimination of these low-frequency signals from the low-frequency signals of the background is impossible in most cases using the traditional methods [35]. The geochemistry traditional methods cannot properly identify the buried mineral deposits, especially in the areas with weak mineralization outcrops and thick overburden. Therefore, detecting these geochemical patterns and signatures of deep mineralization is an important goal that is related to the mineralization processes and migration mechanisms. There is no distinct and unit idea about the migration processes of geochemical elements in covered mineral deposits [35, 36]. The weak geochemical signals can be caused at the surface due to the elemental migration of deep and covered mineral deposits. The quantitative approaches are required for investigation of these weak anomalies and migration process. The buried and deep ore deposits commonly have a weaker elemental concentration at the surface rather than the areas with mineralization outcrops and surface ore deposits [37]. Cheng (2012) has illustrated a deep deposit with a depth of around 1 km; unlike the surface outcropped deposits, it created weak Sn concentrations at the surface containing the low-frequency signals, the same as the regional background component. The mineralization elements of the deep buried resources show low surficial geochemical signatures, and discriminating these weak geochemical anomalies from the high background component is so hard [35]. In some covered areas, separation of the low anomaly from the high background that have been mixed and superimposed is very difficult [37]. The geochemical data formed by various mixed geological processes should be decomposed using the novel sophisticated computational approaches [36, 37]. Cheng (2012) has shown that the superficial mineral deposits cause the high surface

anomalies and the hidden and deep mineral deposits to create weak anomalies at the surface [37]. Mahdianfar (2019) has shown that the hidden and deep mineralizations create a geochemical distribution map at the surface with a weak intensity and low variability (i.e. low-frequency signals) that may be the same as the background values. He demonstrated that the deep mineral deposits cause a weak surface anomaly with low-frequency signals at the surface [20]. The weak surface anomaly may not be distinguishable properly from the background component. In these cases, the surface geochemical distribution map of the mineralization elements shows a weak concentration with low-frequency signals, the same as the background map. Zuo and Wang (2015) have presented the simulated deep mineral deposit models with various depths in order to show the distribution map of the frequency signals at the surface. They demonstrated that very deep deposits create low surface concentrations with low-frequency signals that have been superimposed on the background component. They obviously showed in this cases that the geochemical patterns such as the mineralization processes and background component are indistinguishable, and that the geochemical anomaly cannot be detected using the concentration-area and S-A fractal methods [11]. Shahi *et al.* (2015) have shown that the deep mineralization elements can be identified using the low-frequency geochemical signals extracted from a surface geochemical distribution map [18].

5. Sampling and analytical methods

The distribution maps of the geochemical samples in these areas are depicted in Figure 2. 165 soil samples on a network with distances of 50 m were collected from the Dalli area, and these samples with a size fraction of -200 mesh were analyzed using the ICP-MS method in the Amdel laboratory in Australia [30]. In the Tanurcheh area, 104 lithochemical samples were collected from the alteration zones and mineralization outcrops in several stages in order to study the assay of gold, copper, and 24 other elements. These samples were analyzed using the ICP method in OMAC at Ireland and ALS CHEMEX at Canada [34]. In the Zafarghand area, 177 lithochemical samples were collected and analyzed for 36 elements using the ICP-MS method in the Amdel laboratory in Australia [32].

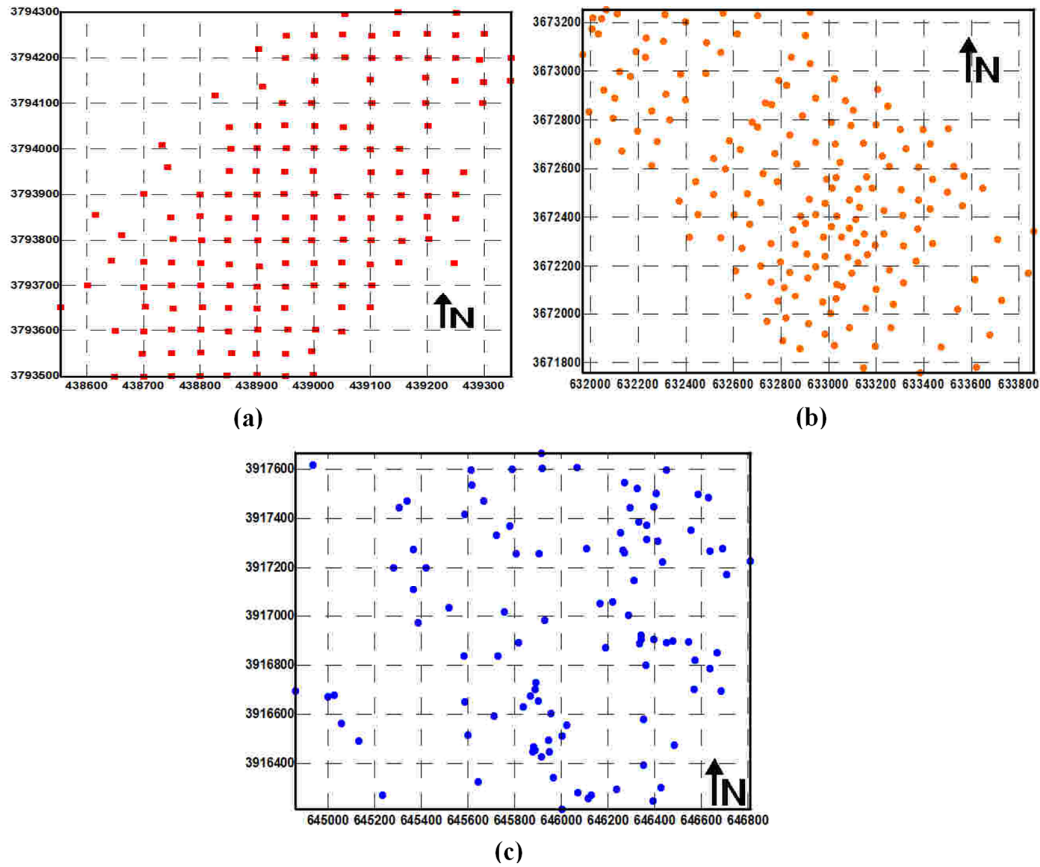


Figure 2. Distribution maps of the geochemical samples from the Dalli area (A), Zafarghand area (B), and Tanurcheh area (C).

6. Results and Discussion

Various aspects of the geochemical FD data can be considered for recognition of the complex geochemical patterns and extraction of new exploratory information. In this section, a novel criterion in FD is proposed in order to distinguish the deep mineralization zones and the deep non-

mineralization zones. Three different mineralization areas with thick overburden consisting of the Dalli, Zafarghand, and southern Tanurcheh mineralization areas were surveyed for discussion. The statistical attributes of the mineralization elements at the surface in the studied areas are shown in Table 1.

Table 1. Statistical attributes of the mineralization elements in the studied areas based on the surface geochemical data.

Number of samples	Southern Tanurcheh		Dalli		Zafarghand	
	104		165		177	
Number of analyzed elements	26		30		36	
Mineralization elements	Au	Cu	Au	Cu	Cu	Mo
Max.	11.48	552	2.87	5403	17002	89.6
Min.	0.02	9	0.01	49	2	0.88
Mean	0.97	123	0.29	871.44	190.79	6.24
Median	0.40	95.50	0.04	343	41	1.09
Std.	2.17	117.17	0.49	1055	1281.14	13.32
Variance	4.72	13728	0.2	1113033	1641328	177.4
Skewness	4.32	1.87	2.4	1.77	12.99	3.95
Kurtosis	20.2	5.09	6.7	2.99	171.25	18.07

The Dalli Cu-Au porphyry and the Zafarghand Cu-Mo porphyry ore deposits are known as the

deep mineralization zones, while the Tanurcheh Cu-Au porphyry mineralization area does not show

a notable mineralization at high depths on the basis of drilled boreholes. The distribution maps of the

surface geochemical anomaly for these areas are depicted in Figure 3.

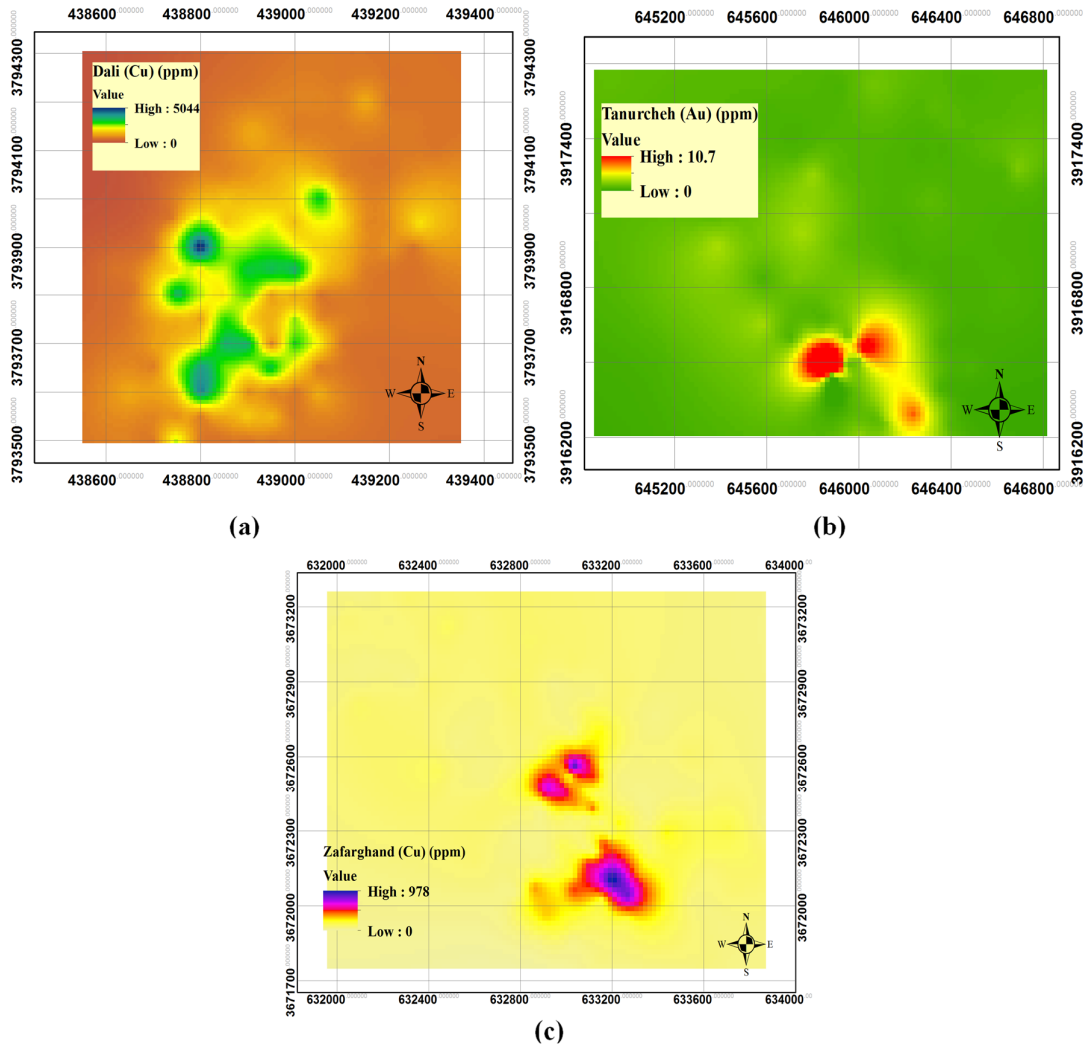


Figure 3. Surface geochemical anomaly maps of the three mentioned case studies.

Two different types of filter functions can be designed in the FD of geochemical data including the PS-based and wavenumber-based filters. The PS-based filter is applied only on the PS values without considering the wavelengths and wave numbers, and divides them into several classes. The applied filters in the S-A fractal method are on the basis of the PS values. The wavenumber-based filters are designed on the basis of the wave number and wavelength values, and include the low band and high pass filters. In these filters, certain frequency signals are eliminated and some frequency signals are enhanced based on the amount of wave numbers in the Kx-Ky map [19, 20]. These two types of filter functions have been utilized in order to interpret the low-frequency signals and identify the geochemical patterns.

Zuo et al. (2015) have simulated the ore deposit models with different depths, and have demonstrated that the S-A fractal method and the PS-based filters cannot detect the hidden and deep ore deposits with a thick overburden [20]. The PS maps of the elements have not been deeply analyzed, especially by the advanced mathematical approaches in order to achieve the reality of the geochemical frequency signals and their features until now. There are several important questions that should be discussed for the buried ore deposit detection. Do the deep and buried mineral deposits have no effect on the low-frequency signals in the surface geochemical data? Do the hidden deep ore deposits and the outcropped and superficial deposits have similar frequency behaviors together

and create similar dispersion patterns at the surface?

The weak surface geochemical anomalies of the deep deposits can be combined with the background values and create the complicated geochemical patterns, and hence, identification of the geological phenomena and mineralization processes, especially in the spatial domain, is so difficult [38]. The geological and mineralization processes can be distinguished using interpretation of the frequency behavior of elements in FD that is related to their migration features and variabilities at the surface. Application of data processing approaches associated with the multivariate data analysis methods can be helpful to solve this important issue. This work indicates that deep deposits have different frequency behaviors from the background elements at the surface.

In order to understand the frequency behavior of the deep ore deposits in low-frequency signals the geochemical anomalies were filtered by low-pass filters, and the outputs obtained were analyzed using the PCA multivariate statistical method.

The PS distribution maps of the mineralization elements in three mineralization areas are illustrated in Figure 4. A low-pass filter function that eliminates the frequencies with high and

moderate wave numbers was designed and performed on the K_x - K_y maps of all of elements. This filter preserves the wave numbers less than 0.01 in the horizontal and vertical directions and eliminates other frequencies for all the elements. In order to investigate the relationships between the elements and achieve new information, the PCA method was performed on these low-frequency signals that were obtained by the wavenumber-based filters. This scenario was performed on the geochemical data for three mineralization areas separately. The rotated component matrices of PCA are shown in Table 2.

The low-frequency signals with wave numbers less than 0.01 were separated, and the PCA method was performed on this dataset including the PS values for all of elements. PCA, as a powerful multivariate method, can be helpful to determine the independent factors and their features. The share and effect of any variable (in this case, the elements) in the PCs obtained can be quantified and the various hidden patterns in the dataset can be revealed. The geochemical dataset is a superimposition of different geological processes and mineralization mechanisms. PCA can distinct these independent patterns and characterize their effective elements.

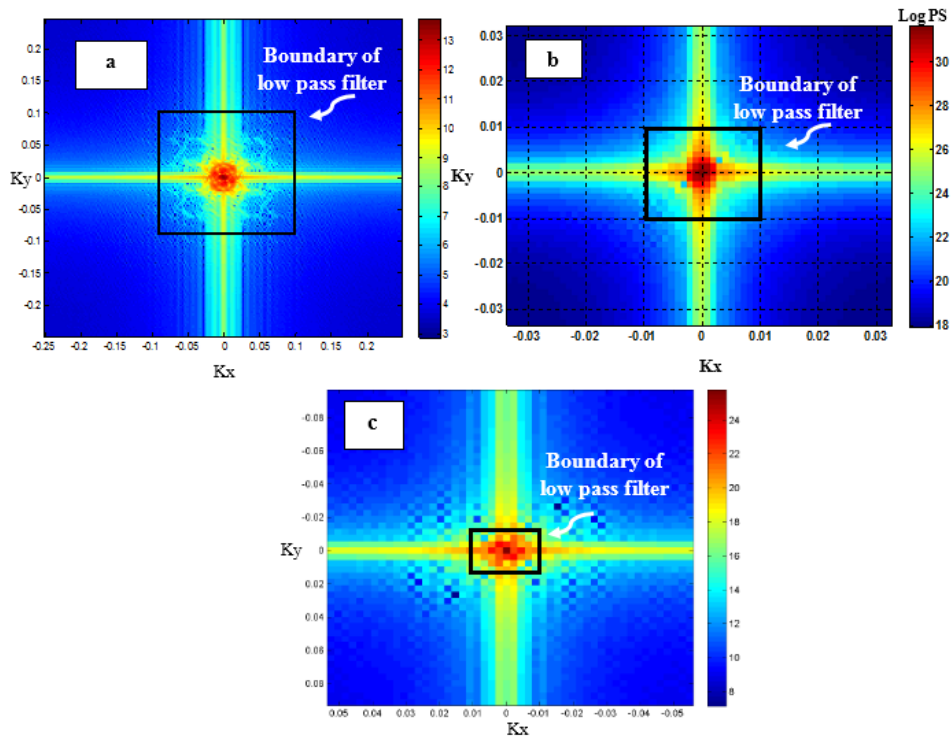


Figure 4. PS maps obtained by FT and schematic boundaries of the designed low-pass filter a: Dalli area, Au; b: Zafarghand area, Cu; c: Tanurcheh area, Cu.

In the Dalli area, PCA has reduced 30 elements into two components (Table 2). The intense

dimension reduction of the variables indicate that there are clear and distinct patterns in this data.

Two distinct geochemical patterns were extracted from PCA. The mineralization elements consisting of Au, Cu, Mo, and S are clearly shown in the second component as the mineralization factor and

are separated from the other elements. PC1 containing the other elements is related to the background factor.

Table 2. Rotated component matrices of PCA on the low-frequency signals showing that the independent components are related to the mineralization and background processes.

	Dalli		Zafarghand		Tanurcheh			
	Component		Component		Component			
	1	2	1	2	1	2		
Au	0.49	0.80	Au	0.54	0.83	Au	0.69	0.65
Al	0.94	0.33	Al	0.94	0.34	Al	0.65	0.71
As	0.91	0.40	Ca	0.90	0.42	As	0.88	0.40
B	0.93	0.36	Fe	0.89	0.46	Ba	0.92	0.36
Ba	0.94	0.34	K	0.91	0.42	Ca	0.95	0.31
Ca	0.89	0.44	Mg	0.92	0.38	Ce	0.96	0.29
Ce	0.94	0.33	Na	0.93	0.37	Co	0.94	0.32
Co	0.94	0.34	Ag	0.81	0.59	Cr	0.88	0.46
Cr	0.94	0.35	As	0.70	0.72	Cu	0.93	0.34
Cu	0.59	0.77	Ba	0.89	0.45	Fe	0.95	0.30
Fe	0.94	0.33	Be	0.94	0.34	K	0.46	0.80
Ga	0.94	0.33	Bi	0.36	0.93	La	0.95	0.29
K	0.94	0.33	Cd	0.88	0.46	Mg	0.76	0.64
La	0.94	0.33	Ce	0.93	0.38	Mn	0.94	0.33
Li	0.94	0.35	Co	0.87	0.48	Mo	0.81	0.48
Mg	0.94	0.33	Cr	0.38	0.78	Na	0.47	0.82
Mn	0.94	0.35	Cs	0.95	0.33	Ni	0.82	0.53
Mo	0.07	0.96	Cu	0.25	0.97	P	0.94	0.35
Na	0.94	0.34	La	0.93	0.37	Pb	0.49	0.69
Ni	0.92	0.39	Li	0.91	0.42	S	-0.07	0.88
P	0.94	0.33	Mn	0.89	0.45	Sc	0.86	0.48
Pb	0.94	0.34	Mo	0.45	0.88	Sr	0.82	0.51
S	0.59	0.72	Nb	0.94	0.35	Ti	0.56	0.80
Sc	0.94	0.34	Ni	0.67	0.67	V	0.75	0.64
Sr	0.93	0.37	P	0.94	0.34	Y	0.88	0.46
Ti	0.94	0.34	Pb	0.06	0.97	Zn	0.92	0.36
V	0.94	0.34	Rb	0.93	0.37			
Y	0.94	0.33	S	0.53	0.69			
Zn	0.94	0.33	Sb	0.95	0.32			
Zr	0.93	0.36	Sc	0.94	0.34			
			Th	0.93	0.36			
			Ti	0.94	0.34			
			W	0.94	0.34			
			Yb	0.93	0.37			
			Zn	0.75	0.66			
			Zr	0.93	0.37			

These results obviously demonstrate that there are strong effects of the mineralization process in the low surface frequency signals of deep ore deposits. The deep ore deposits with thick overburden layers can create the low-frequency geochemical signals at the surface.

The drilled borehole in the area indicates various mineralizations such as hematite, goethite, malachite, bornite, and native Cu at different depths. The PC mineralization obtained has a good correspondence with the deep mineralization

process, and has properly separated the deep mineralization elements from the other elements.

PCA has also divided the 36 elements in the Zafarghand area into two components consisting of the mineralization factor and the background factor. The elements Au, Cu, Mo, As, Bi, Cr, S, and Ni have been perfectly separated in the mineralization component (Table 2). The mineralization pattern and the effects of the mineralization process are strongly shown in the low-frequency signals in this deep mineralization

area with a thick overburden. In the covered deeply mineralized zones, the low-frequency geochemical signals of the surface distribution map are affected by the background component and deep mineralization elements. The deep ore deposits with a thick overburden, particularly those without significant outcrops create the surface geochemical anomalies with low variabilities and low frequency signals, the same as the background geochemical signals, which can be distinguished by the mathematical multivariate methods.

The distinct mineralization pattern is not shown in the PCA results obtained from the Tanurcheh area (Table 2). The mineralization elements Au and Cu in the Tanurcheh area were separated in component 1 as the background factor. The deep boreholes drilled in this area did not show any

mineralization zone at high depths. This mentioned area holds relatively great mineralization outcrops, while includes a non-mineralized zone at high depths. The frequency behavior of the mineralization elements in the Tanurcheh area is completely different from the blind mineralization zones in Dalli and Zafarghand that are associated with deep mineralization zones, and are known as the economic deep mineralization areas.

A novel diagram as a differentiating criterion on the basis of the obtained PCs is proposed in order to distinguish the deep mineralization zones from the non-mineralization areas (Figure 5). The scores of the mineralization elements in PCs of PCA were plotted, and the positions of the mineralization elements for three areas were illustrated in this figure.

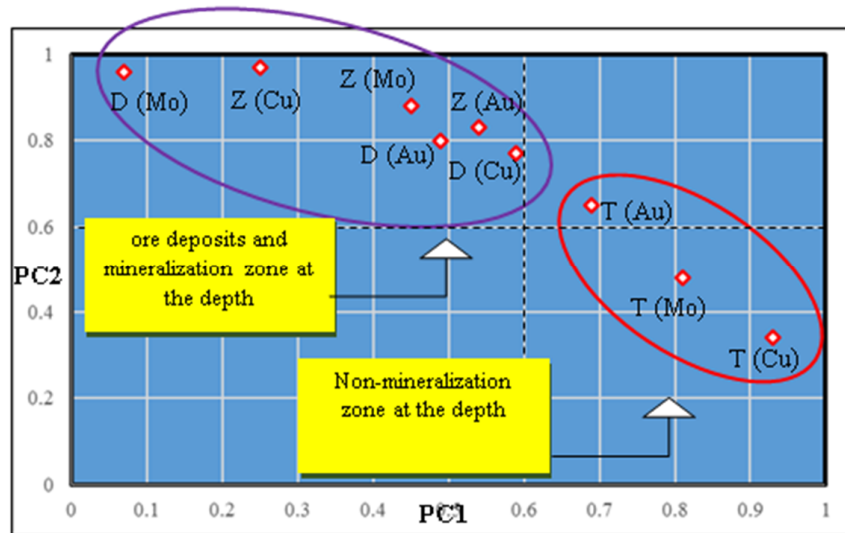


Figure 5. Proposed diagram based on the PCA results of geochemical filtering that classifies the hidden ore deposits and non-mineralized zones.

The positions of the Au, Mo, and Cu elements in Tanurcheh (T(Au), T(Mo), and T(Cu)), and Zafarghand (Z(Au), Z(Mo) and Z(Cu)), Dalli (D(Au), D(Mo), and D(Cu)) are depicted in this figure. The mineralization elements of the buried ore deposits were completely separated from the elements in the deep non-mineralization area based on the behavior of the elements in FD. The three case studies were perfectly classified into the two deep mineralization and deep non-mineralization zones. The coefficients of elements in PC2 for the three mineralization areas are depicted in Figure 6. This figure shows the role and importance of the elements in the mineralization factor. The frequency behaviors of the elements in the Dalli

and Zafarghand areas are similar. The values of the mineralization elements Cu, Mo, Au, and S in these two areas are bigger than the threshold of 0.6. The effective elements on this PC in the Tanurcheh area are different from the mineralization elements in the Dalli and Zafarghand areas. The frequency behavior of the elements in the background factor (PC1) for the Dalli, Tanurcheh, and Zafarghand areas is depicted in Figure 7. Most elements in the Dalli and Zafarghand areas behave similar to each other. In the Tanurcheh area, the elements Cu, Au and Mo hold the important role in this PC (background factor), unlike the Dalli and Zafarghand areas.

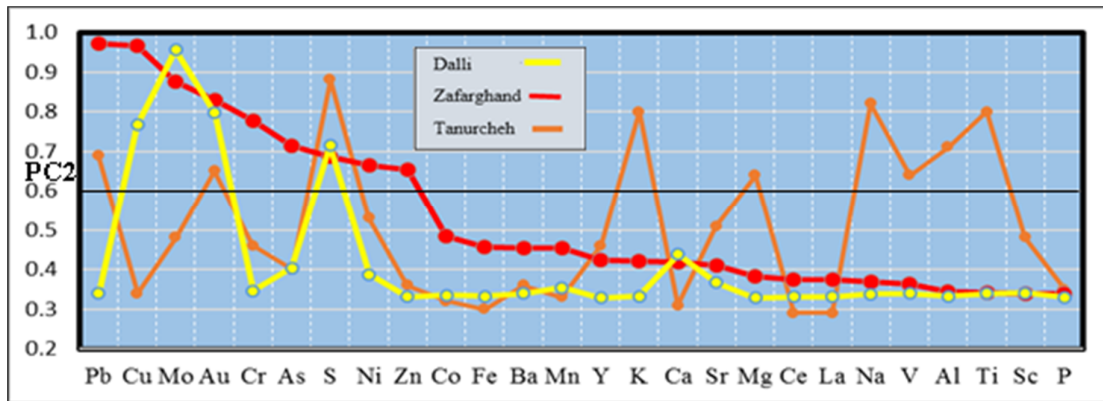


Figure 6. Frequency behavior of the elements in the mineralization factor (PC2) for the Dalli, Tanurcheh, and Zafarghand areas.

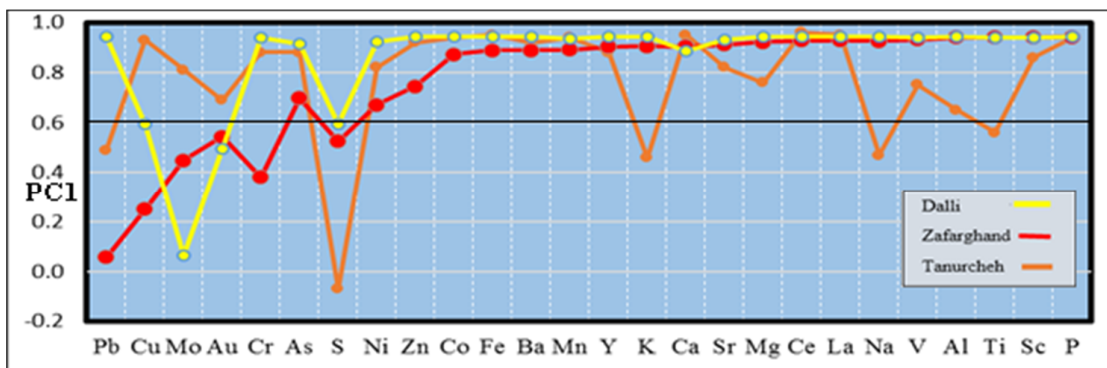


Figure 7. Frequency behavior of the elements in the background factor (PC1) for the Dalli, Tanurcheh, and Zafarghand areas.

The vertical distribution of the mineralization elements at the depth by drilled boreholes strongly correspond to the results obtained (Figure 8). The drilled boreholes show that there is a non-mineralized zone at the high depth in the Tanurcheh area, and indicate that the Dalli and Zafarghand areas are from the true anomaly type and hold hidden mineralized zones at the depth. Three mineralized zones consisting of supergene (e.g. Malachite, Hematite, and Goethite), transition (e.g. native Cu), and hypogene (e.g. Bornite) at different depths have been explored in the Dalli area. In the Zafarghand area, various exploration layers consisting of the Cu-Mo geochemical anomaly maps, a strong

IP-RS anomaly map, a phyllic alteration map, and quartz stockwork and Fe oxides maps were employed in order to determine the location of boreholes. The geophysics profiles on the Cu anomaly area show deep strong anomalies that are associated with the sulfide zones at the depth. The drilled borehole indicates that there is a mineralized zone at the depth (Figure 8). The proposed approach demonstrates that the low-frequency geochemical signals at the surface are indeed a combination of the effects of the deep mineralization zones and the background component. This sophisticated method can quantitatively distinguish the deep mineralized and non-mineralized zones.

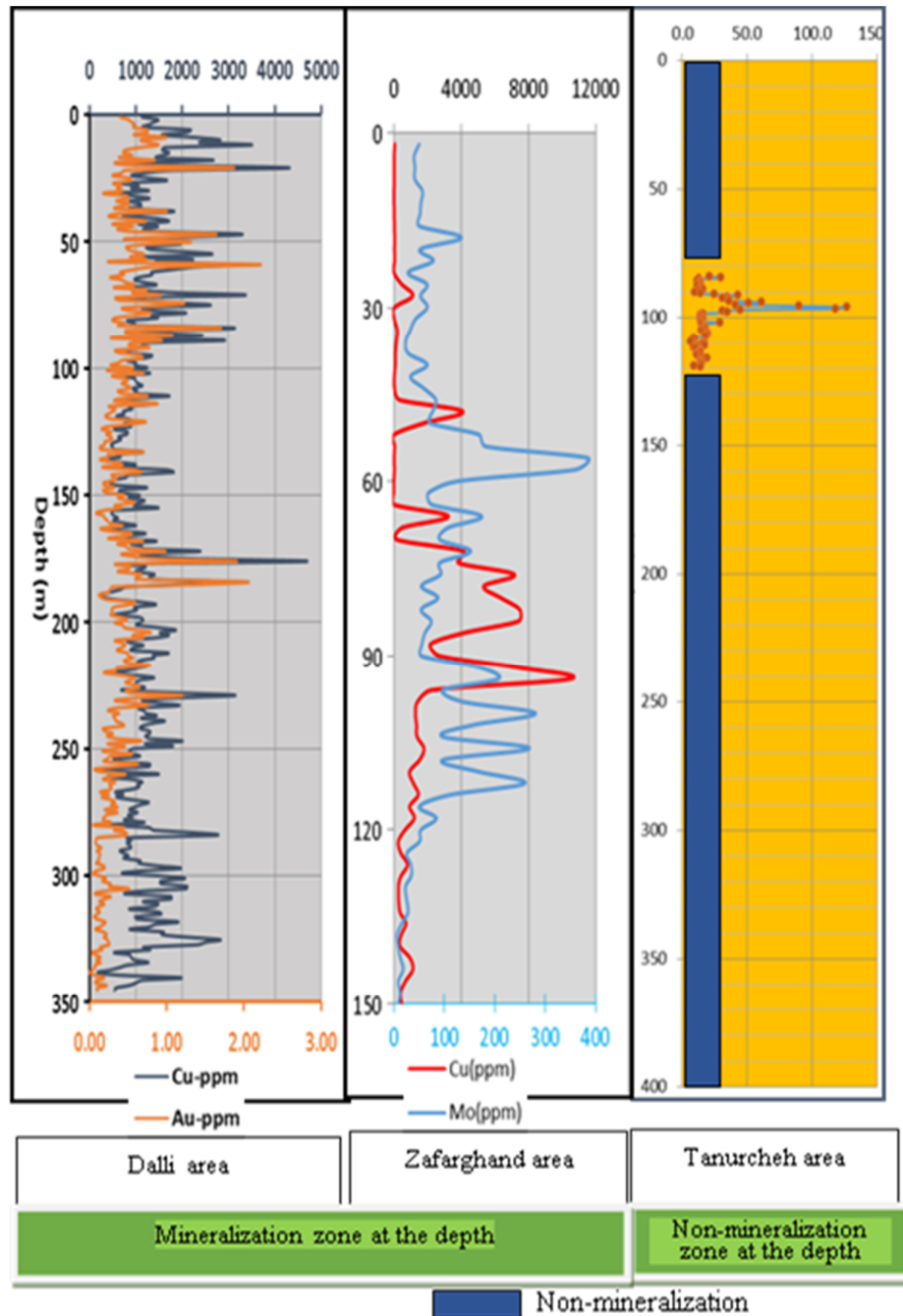


Figure 8. Vertical distribution of the mineralization elements by drilled boreholes showing the deep non-mineralized zone in the Tanurcheh area and the deep mineralized zone in the Dalli and Zafarghand areas.

The combined PCA and geochemical anomaly filtering approach can provide information about the mineralization zones and the geochemical patterns at the depth, especially in the buried deposits with a thick overburden. This combined approach including PCA and anomaly filtering is proposed as an effective tool for prediction of the deep mineralization elements and identification of the buried ore deposits that may be hidden and undiscovered in the exploratory studies.

7. Conclusions

In this work, the wavenumber-based filter function was applied for the geochemical anomaly filtering. The wavenumber-based filter was done on the power spectrum distribution map in the three case studies of the Dalli, Zafarghand, and Tanurcheh mineralization areas, and the wave numbers less than 0.01 were separated and analyzed using PCA. The results obtained indicate

that there are strong effects of the mineralization process on the low-frequency signals. The deep buried ore deposits (Dalli and Zafarghand) were properly discriminated from the deep non-mineralized Tanurcheh area using a new diagram on the basis of the scores of the mineralization elements in the principal factors obtained. The drilled boreholes thoroughly confirmed the results obtained. This effective scenario demonstrates that the low-frequency signals of geochemical data hold new important exploratory information.

The proposed approach demonstrates that the low-frequency geochemical signals at the surface data are affected by the deep ore deposits and the background factor.

References

- [1]. Sifuzzaman M., Islam M. R., and Ali M.Z., 2009. Application of wavelet transform and its advantages compared to Fourier transform.
- [2]. Cheng Q., Xu Y., Grunsky E., 1999. Integrated spatial and spectrum analysis for geochemical anomaly separation. In: Proc. Intern. Assoc. for Math. Geology Meeting, S. J. Lippard, A. Naess, and R. Sinding-Larsen eds., Trondheim, Norway, 1: 87-92.
- [3]. Cheng Q., Xu Y., and Grunsky E., 2000. Integrated Spatial and Spectrum Method for Geochemical Anomaly Separation, Natural Resources Research, Vol. 9, No. 1.
- [4]. Parsa, M., Maghsoudi, A., Yousefi, M., and Sadeghi, M., 2017. Multifractal analysis of stream sediment geochemical data: Implications for hydrothermal nickel prospecting in an arid terrain, eastern Iran. *Journal of Geochemical Exploration*, 181, pp. 305-317.
- [5]. Roshanravan B., Tabatabaei S.H., Kreuzer O., Moini H., and Parsa M., 2020. Structural and non-structural statistical methods: implications for delineating geochemical anomalies. *Applied Earth Science*. 129 (3): pp. 111-121.
- [6]. Koohzadi F., Afzal P., Jahani D., and Pourkermani M., 2020. Geochemical exploration for Li in regional scale utilizing Staged Factor Analysis (SFA) and Spectrum-Area (S-A) fractal model in north central Iran. *Iranian Journal of Earth Sciences* (In press).
- [7]. Cao L., Cheng Q., 2012. Quantification of anisotropic scale invariance of geochemical anomalies associated with Sn-Cu mineralization in Gejiu, Yunnan Province, China, *Geochemical Exploration* 122: 47–54.
- [8]. Saljoughi B.S., Hezarkhani A., 2019. Identification of geochemical anomalies associated with Cu mineralization by applying spectrum-area multi-fractal and wavelet neural network methods in Shahr-e-Babak mining area, Kerman, Iran. *Journal of Mining and Environment*. 10 (1): 49-73.
- [9]. Zuo R., Carranza E.J.M, and Cheng Q., 2012. Fractal/multifractal modelling of geochemical exploration data. *Journal of Geochemical Exploration* 122, 1-3.
- [10]. Zuo R., Xia Q., Zhang D., 2013. A comparison study of the C-A and S-A models with singularity analysis to identify geochemical anomalies in covered areas. *Applied Geochemistry* 33, 165-172.
- [11]. Zuo R., Wang J., 2015. Fractal/multifractal modeling of geochemical data: A review. *Journal of Geochemical Exploration*.
- [12]. Ghezelbash R., Maghsoudi A., and Daviran M., 2019. Combination of multifractal geostatistical interpolation and spectrum–area (S–A) fractal model for Cu–Au geochemical prospects in Feizabad district, NE Iran. *Arabian Journal of Geosciences*. 12 (5): 152.
- [13]. Maghsoudi A., Yousefi M., and Carranza E.J.M., 2017. Multifractal interpolation and spectrum–area fractal modelling of stream sediment geochemical data: implications for mapping exploration targets. *Journal of African Earth Sciences*, 128, 5-15.
- [14]. Zuo R., 2011. Identifying geochemical anomalies associated with Cu and Pb–Zn skarn mineralization using principal component analysis and spectrum–area fractal modeling in the Gangdese Belt, Tibet (China). *Journal of Geochemical Exploration*. 111 (1-2): 13-22.
- [15]. Wang H., Zuo R., 2015. A comparative study of trend surface analysis and spectrum–area multifractal model to identify geochemical anomalies. *Journal of Geochemical Exploration*. 155: 84-90.
- [16]. Afzal P., Fadakar Alghalandis Y., Moarefvand P., Rashidnejad Omran N., and Asadi Haroni, H., 2012. Application of power-spectrum-volume fractal method for detecting hypogene, supergene enrichment, leached and barren zones in Kahang Cu porphyry deposit, Central Iran, *Journal of Geochemical Exploration* 112, 131–138.
- [17]. Khalili H., Afzal, P., 2018. Application of spectrum-volume fractal modeling for detection of mineralized zones. *Journal of Mining and Environment* 9: 371-378.
- [18]. Shahi H., Ghavami Riabi R., Kamkar Ruhani A., and Asadi Haroni H., 2015. Prediction of mineral deposit model and identification of mineralization trend in depth using frequency domain of surface geochemical data in Dalli Cu-Au porphyry deposit. *Journal of Mining and Environment*. 6 (2): pp. 225-236.
- [19]. Shahi H., Ghavami. R., Rouhani A.K., 2016. Detection of deep and blind mineral deposits using new proposed frequency coefficients method in frequency domain of geochemical data. *Journal of Geochemical Exploration*.
- [20]. Mahdianfar H., 2019. Detection of Mo geochemical anomaly in the depth using a new scenario

based on the spectrum–area fractal analysis. *Journal of Mining and Environment*, DOI: 10.22044/JME.2019.7944.1662.

[21]. Johnson R.A., Wichern D.W., 2002. *Applied multivariate statistical analysis* (Vol. 5, No. 8). Upper Saddle River, NJ: Prentice hall.

[22]. Parsa M., Maghsoudi A., Carranza E.J.M., and Yousefi M., 2017. Enhancement and mapping of weak multivariate stream sediment geochemical anomalies in Ahar Area, NW Iran. *Natural Resources Research*. 26 (4): pp. 443-455.

[23]. Lisitsin V., 2015. Spatial data analysis of mineral deposit point patterns: Applications to exploration targeting. *Ore Geology Reviews*, 71, pp. 861-881.

[24]. Parsa M., Maghsoudi A., and Yousefi M., 2018. Spatial analyses of exploration evidence data to model skarn-type copper prospectivity in the Varzaghan district, NW Iran. *Ore Geology Reviews*, 92, pp. 97-112.

[25]. Jolliffe I.T. and Cadima, J., 2016. Principal component analysis: a review and recent developments. *Philosophical Transactions of the Royal Society A: Mathematical, Physical and Engineering Sciences*. 374 (2065): p. 20150202.

[26]. Naik G.R. ed., 2017. *Advances in Principal Component Analysis: Research and Development*. Springer.

[27]. Cios K.J., Swiniarski R.W., Pedrycz W., and Kurgan L.A., 2007. *The knowledge discovery process*. Data Mining. Springer, US, pp. 9–24.

[28]. Dobrin M.B., Savit C. H., 1988. *Geophysical prospecting*: McGraw-Hill Book Co., New York, 867 p.

[29] Shahi H., Ghavami R., Kamkar Rouhani A., and Asadi-Haroni H., 2014. Identification of mineralization features and deep geochemical anomalies using a new FT-PCA approach, *Journal of Geopersia*, 4 (2): 101-110.

[30]. Darabi-Golestan F., Ghavami-Riabi R., and Asadi-Harooni H., 2013. Alteration, zoning model, and mineralogical structure considering lithochemical investigation in Northern Dalli Cu–Au porphyry. *Arabian Journal of Geosciences*, 6 (12): 4821-4831.

[31]. Asadi Haroni H., 2008. *First Stage Drilling Report on Dalli Porphyry Cu-Au Prospect, Central Province of Iran*, Technical Report.

[32]. Asadi Haroni H., 2013. *Preliminary Exploration at Zafarghand Porphyry Copper Property, Central Iran*.

[33]. Farzamian M., Rouhani A.K., Yarmohammadi A., Shahi H., Sabokbar H.F., and Ziaie M., 2016. A weighted fuzzy aggregation GIS model in the integration of geophysical data with geochemical and geological data for Pb–Zn exploration in Takab area, NW Iran. *Arabian Journal of Geosciences*, 9 (2): 104.

[34]. Karimpour M., 2004. *Geological report of Tanurcheh mineralization area*, Zarmehr Company.

[35]. Cheng Q., 2014. Vertical distribution of elements in regolith over mineral deposits and implications for mapping geochemical weak anomalies in covered areas. *Geochemistry: Exploration, Environment, Analysis*, 14 (3): 277-289.

[36]. Cohen D.R., Kelley D.L., Anand R., and Coker W.B., 2010. Major advances in exploration geochemistry, 1998–2007. *Geochemistry: Exploration, Environment, Analysis*, 10 (1): 3-16.

[37]. Cheng Q., 2012. Singularity theory and methods for mapping geochemical anomalies caused by buried sources and for predicting undiscovered mineral deposits in covered areas. *Journal of Geochemical Exploration*, 122, 55–70.

[38]. Lin J., Kang L., Liu C., Ren T., Zhou H., Yao Y., and Zhang M., 2019. The frequency-domain airborne electromagnetic method with a grounded electrical source. *Geophysics*, 84 (4): 1-43.

شناسایی ذخایر معدنی فلزی مدفون با استفاده از فیلتر کردن آنومالی ژئوشیمیایی و فاکتورهای اصلی طیف توان

حسین مهیدیان فر*

گروه مهندسی معدن، مجتمع آموزش عالی گناباد، ایران

ارسال ۲۰۲۰/۰۹/۲۹، پذیرش ۲۰۲۰/۱۲/۰۴

* نویسنده مسئول مکاتبات: hssn.shahi@gmail.com

چکیده:

در طول دو دهه گذشته حوزه فرکانس داده های ژئوشیمیایی به وسیله برخی از محققین مورد مطالعه قرار گرفته است. منطقه بندی فلزی یکی از موضوعات چالشی در اکتشاف معدن است که یک سناریوی جدید در حوزه فرکانس برای حل این مشکل پیشنهاد شده است. سه منطقه کانی سازی شامل منطقه کانی سازی مس-طلائی دالی، منطقه کانی سازی مس-مولیبدن ظرفرند و منطقه کانی سازی مس-طلائی تنورچه برای این تحقیق انتخاب شده اند. بعد از انتقال داده های ژئوشیمی سطحی به حوزه فرکانس، سیگنال های ژئوشیمیایی حاصل با استفاده از فیلترهایی بر مبنای عدد موج فیلتر می شوند. سیگنال های فرکانسی متوسط و بالا حذف شده و سیگنال های باقی مانده با استفاده از روش آماری تحلیل مولفه های اصلی مورد تفسیر قرار می گیرند. به منظور تمایز بین ذخایر معدنی عمیق فلزی، فاکتورهای اصلی طیف توان عنصری بدست آمده بوسیله روش تحلیل مولفه های اصلی، در یک نمودار جدید (مولفه اصلی اول در مقابل مولفه اصلی دوم) ترسیم می شوند. این روش نشان می دهد که داده های ژئوشیمیایی در ذخایر معدنی عمیق دالی و ظرفرند رفتارهای فرکانسی مشابهی دارند. عناصر طلا، مولیبدن و مس در این دو منطقه از عناصر کانی سازی طلا، مولیبدن و مس منطقه تنورچه به عنوان یک منطقه فاقد کانی سازی عمیق در این نمودار متمایز می شوند. این معیار جدید جهت متمایز کردن ذخایر معدنی مدفون و مناطق فاقد کانی سازی عمیق به طور مناسبی به وسیله گمانه های عمیق اکتشافی حفر شده تایید می شود. فیلتر کردن آنومالی ژئوشیمیایی نشان می دهد که علائم قوی از کانی سازی عمیق با سیگنال های فرکانسی پایین ژئوشیمیایی در سطح همراه هستند و مناطق کانی سازی مدفون با آنومالی ضعیف سطحی می توانند با استفاده از داده های حوزه فرکانس ژئوشیمیایی شناسایی شوند.

کلمات کلیدی: فیلتر کردن آنومالی ژئوشیمیایی، ذخیره مدفون، فیلتر بر مبنای عدد موج، طیف توان.